Hydrodynamic studies of two-phase liquid-liquid slug flow in circular microchannel with T-junction

Aloisiyus Yuli Widianto ✉; Caroline Elfa; Reynaldo Valentino
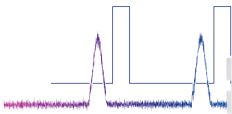
Check for updates

View Online   Export Citation   CrossMark

Hydrodynamic Studies of Two-Phase Liquid-Liquid Slug Flow in Circular Microchannel with T-Junction

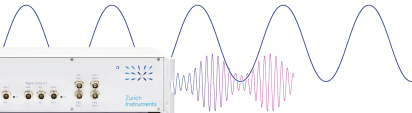Aloisiyus Yuli Widianto[1, a)], Caroline Elfa[1, b)], Reynaldo Valentino[1, c)]

[1]*Chemical Engineering-University of Surabaya, Jl. Raya Kalirungkut, Surabaya, Indonesia*

[a)]*Corresponding Author: aloy_sius_yw@staff.ubaya.ac.id*
[b)]*s160216004@student.ubaya.ac.id*
[c)]*s160216021@student.ubaya.ac.id*

Abstract. Microreactors are widely applied, especially in heterogeneous reactions limited by mass and or heat transfer. In many chemical reactions, microreactors perform well in obtaining a high yield, selectivity, and conversion up to 100%, which is not easy to realize using conventional reactors. The excellent performance results from the high stability of the two-phase flow, namely slug flow pattern. A comprehensive study of slug flow characteristics inside the microchannel is needed to have a good performance. For that reason, the present work focused on the study of slug flow characteristics and its stability by using a circular microtube with 0.5, 0.8, and 1 mm inside diameter, and the 2-liquid phase consisted of aquades-kerosene and aquades-ethyl acetate with aquades as a dispersed phase and kerosene or ethyl acetate as a continuous phase. These liquids represent two liquid mixtures with different physical and chemical properties, significantly influencing the formation of 2-phase flow patterns in a microtube. Variables used in the experiment were temperature, channel diameter, and volumetric flow rate. Observation results show that the slug flow pattern was found at the ratio of the volumetric flow rate of disperse phase to the continuous phase (Q_d/Q_c) is 1; 1.4; 1.8; and 2.2. The slug flow formed at a flow rate of 70 ml/h for both the dispersed phase and the continuous phase ($Q_d/Q_c = 1$) had the most stable droplet length and the distance of consecutive droplets. Increasing Q_d/Q_c ratio increases the droplet length formed, and in the range of discharge used, the change in inside tube diameter from 0.5 to 1 mm does not change the flow pattern model, but it affects the slug length.

INTRODUCTION

A *Microreactor* is a novel chemical reactor technology that performs excellently in conducting a chemical reaction. This technology in many chemical synthesis applications, mainly for heterogeneous systems, has produced high yields and reaction conversions of up to 100%. One of the main requirements for heterogeneous reactions to take place optimally is the availability of a large contact surface area for mass/heat transfer between phases [1]. On the other hand, currently, the existing conventional reactors can only provide a contact surface area (expressed as specific surface = A/V) up to 400 m^2/m^3, far below the specific surface that can be generated by a microreactor which can reach 40.000 m^2/m^3 in the range channel diameter of 10 μm – 1 mm.

Another excellent performance is shown concerning the hazardous and toxic chemicals applications. In industrial chemical processes, the product of the chemical reaction that involves small volumes has prevented and avoided the risks posed by the use of hazardous and toxic materials in the process. The availability of a substantial specific surface in the miniaturization system of a reactor has facilitated a mass/heat transfer process; therefore, the risk of work accidents, such as explosions due to heat accumulation in a reactor, can be prevented, even the high reaction selectivity which is difficult to achieve with conventional reactors can be realized easily by using this technology. The large specific surface in a microreactor has made it very suitable for applications in highly exothermic or endothermic processes that are limited by mass and or heat transfer, such as the synthesis of organometal, bioethanol dehydration, the synthesis of ethyl methyl oxalate, and many biocatalytic reaction application.

The performance of a two-phase (liquid-liquid) microreactor is principally determined by the flow pattern characteristic and the flow stability formed within a channel. Among the flow patterns type that may develop in a

microchannel, slug is the most stable flow; it has a regular velocity, uniform shape, and distribution. In addition, it has a large specific surface area (*A/V*).

Several factors influenced the formation of flow patterns in a microchannel, including viscosity and density, liquid wettability on the inner wall of a channel, contact angle, surface tension, the flow rate of dispersed and continuous phases, the inner diameter of the channel, and material of the channel. Previous researchers have studied the effect of channel diameter on the flow pattern formed [2][3][4] using PTFE, PMMA, and glass channels [3][4][5]. The effect of liquid-liquid flow rate [5][6][7] with the different types of liquid used to represent the effect of different liquid viscosity [3][4][5][8]. The droplet length and distance between successive droplets on slug flow have been investigated [5]. The studies are still limited to using PTFE, PMMA, and glass tube channel materials and several liquid phases as dispersed/continuous phases. Profound observation using various types of liquid, tube diameter, tube material, and flow rates will enrich existing research results. Understanding the flow pattern characteristics within a microchannel is required to have an optimal result, and it will be a significant consideration in determining the proper microchannel design for a liquid-liquid reaction system. Therefore, this study aims to determine the effect of the flow rate of dispersed and continuous phases, the diameter of a microtube on the flow pattern, the droplet length, and the distance between successive droplets on the slug flow. This study has focused on observing the flow formation within a microchannel (without reaction) by using various channel diameters (silicone), which has yet to be done in previous studies [2][3][5][9,10].

EXPERIMENTAL METHODOLOGY

The experiment was carried out with four variables: the flow rate of the dispersed and continuous phase, the type of liquid two-phase pair, temperature, and microchannel diameter. Variables flow rate and liquid used in the experiment are shown in Tables 1 and 2 below.

TABLE 1. Aquades-kerosene flow rate

Liquid	Flow Rate (ml/h)				
Aquades	25	35	45	55	70
Kerosene	25	25	25	25	70

TABLE 2. Aquades-ethyl acetate flow rate

| Liquid	Flow Rate (ml/h)				
Aquades	25	35	45	55	70
Ethyl acetate	25	25	25	25	70

The experiment was performed at various temperatures of 28, 35, 40, 45, and 50 °C, with 0.5, 0.8 and 1 mm channel diameters and 4.5 m long. The channel used in the experiment is tube silicone (circular microchannel).

Two low discharge syringe pumps delivered the immiscible liquid-liquid two-phase system, Yamamoto Giken YG-80 syringe pump that can deliver liquid phase in the range of 0.1 – 99 ml/h, and Infusia SP7s syringe pump that works with discharge in the range 0.010 – 999 ml/h. The syringe pumps in this observation perform well in dispensing liquids with uniform and stable discharge. The flow pattern was observed with a 12 W LED light and a digital camera (Sony A6000, 50 mm f1.8 lens, and macro tube extension) connected to a computer to easily observe the flow formed. Two computer programs applied are OBS and GIMP. The OBS program was used to observe the flow patterns, and the GIMP was used to measure the dimensions of droplet length and droplet distance.

The principle of the experiment is to make contact with the two-phase liquid-liquid through a T-junction (transparent material) so that the formation of the flow pattern can be observed clearly by using a high-speed digital camera. The experimental setup is shown in Fig. 2.

TABLE 3. Liquid properties

Liquid	Temperature (°C)	Density (kg/m³)	Viscosity (kg/m.s)	Surface Tension (kg/s²)
Aquades	28	996.24	0.836×10^{-3}	0.02375
	35	993.97	0.723×10^{-3}	-
	40	992.25	0.656×10^{-3}	-
	45	995.16	0.599×10^{-3}	-
	50	988.07	0.549×10^{-3}	-
Kerosene	28	803.00	2.200×10^{-3}	0.02000
	35	797.00	1.950×10^{-3}	-
	40	794.00	1.750×10^{-3}	-
	45	791.00	1.600×10^{-3}	-
	50	787.00	1.500×10^{-3}	-
Ethyl acetate	28	890.58	0.450×10^{-3}	0.07280
	35	881.60	0.415×10^{-3}	-
	40	875.50	0.390×10^{-3}	-
	45	869.40	0.370×10^{-3}	-
	50	863.20	0.350×10^{-3}	-
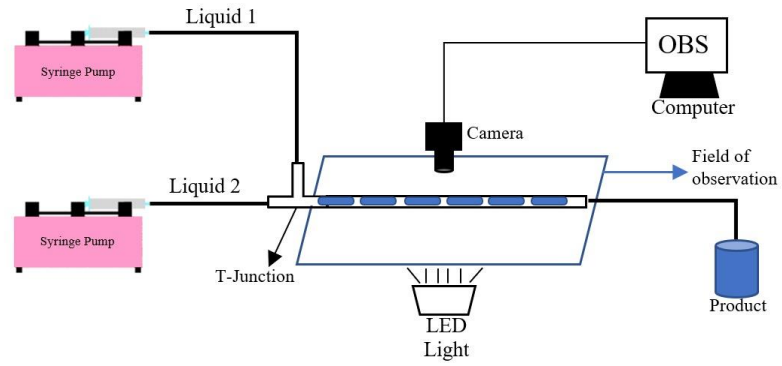
FIGURE 1. Experimental setup [10]

(a)

(b)
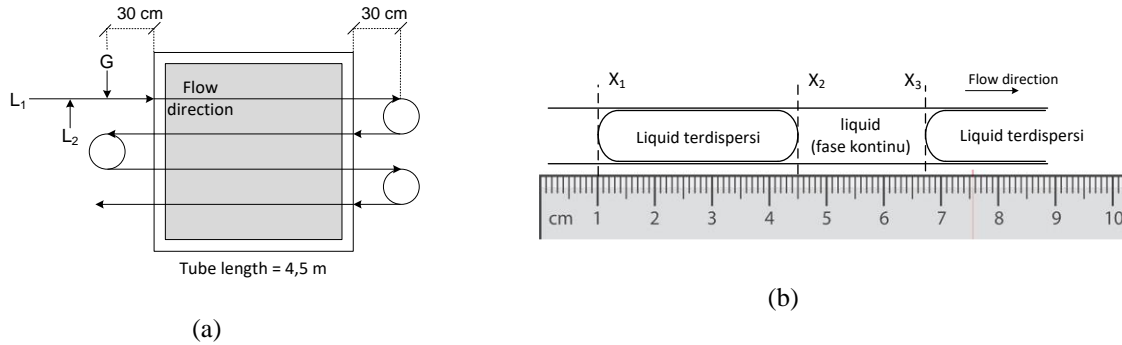
FIGURE 2. (a) The flow pattern observation scheme, (b) The measuring method of droplet length and droplet distance

RESULTS AND DISCUSSION

Liquid-liquid two-phase flow patterns in microtubes can be classified into slug, droplet, thread, jet, and annular flow [9]. From the observations, the slug shows stable flow characteristics with a uniform shape and regular velocity within a microchannel. Slug flow is described as a segmented flow of dispersed liquid in the continuous phase. In a liquid-liquid system, the continuous-phase wrapped slugs around it. High stability flow characteristic with a large surface area contact is a great potential for developing process applications involving mass and or heat transfer, especially highly exothermic and endothermic processes.

Slug formation steps in the liquid-liquid system within a microchannel, i.e., blocking, squeezing, and lag steps, as shown in Fig. 3 [7]. In the blocking step, the continuous and dispersed phases meet at the T-junction; then, the dispersed phase penetrated the main channel, and the slug head grows to fulfill the cross-section of the tube. The squeezing step can be described as the dispersed phase successfully entering the main channel, and the slug tail decreases in size due to the inertial forces of the continuous phase. Lag is one of the steps when droplets have been formed.
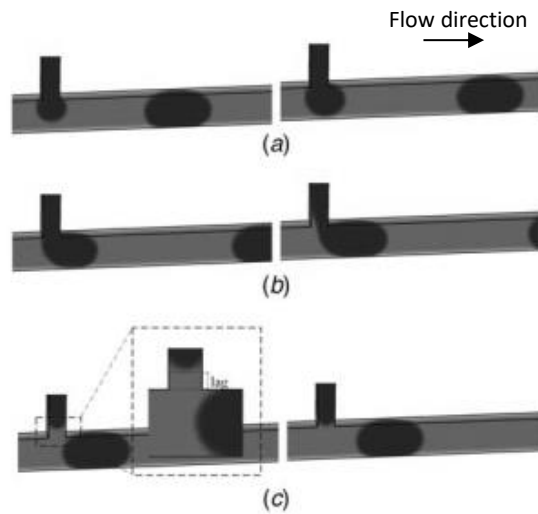

FIGURE 3. Slug flow formation steps
(a) Blocking, (b) Squeezing, (c) Lag [7]

Determination of dispersed and continuous phase rates is important to have the slug flow pattern. The trend observed, if the ratio of dispersed to continuous rate is much less than one, the two-phase flow pattern formed the bubbly flow, and furthermore, if the ratio of dispersed to continuous rate is much higher than one, the annular flow would be formed in the channel. From these observations, the slug was formed when the dispersed and continuous flow rate ratio attained 1; 1.4; 1.8, and 2.2 (Tables 1 and 2).

Liquid-Liquid Two-Phase Flow Pattern-Regime Slug Flow

The slug formation begins at the meeting point of the dispersed and the continuous phase at the T-junction. Fig. 4 shows the slug flow pattern on a microtube with 0.8 mm inside diameter, tube length (L_t) of 4.5 m with a meander channel configuration so that the microtube appeared like to be divided into four rows, with the first channel being the closest to the inlet section.
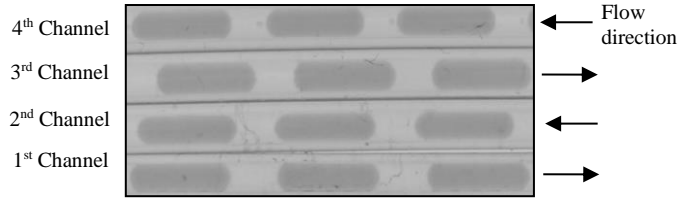
FIGURE 4. Slug flow pattern in Aquades-Kerosene, Q_{aq} = 25 ml/h, Q_{ke} = 25 ml/h, D_t = 0,8 mm, T= 28 °C

The wetting property of liquid is a factor that determines the characteristics of the flow pattern formed. Interactions between the dispersed and the continuous phase with the inner surface of the tube wall determine the formation of a thin liquid film in a narrow space between the droplet and the inner tube wall.

In some previous works on the two-phase liquid-liquid system [2][6], the thin liquid film appeared in the observed system, whereas other studies [3][5][6] cannot detect the appearance of the liquid film within a slug flow pattern. The formation of the thin film is shown in the schematic Fig.5 (b).
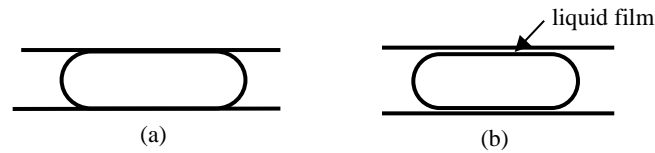

FIGURE 5. (a) Droplet without film, (b) Droplet with film

Experiments using aquades-ethyl acetate formed droplets with a film, whereas in the aquades-kerosene system, liquid droplets formed without a film (Fig. 5(a)). Ethyl acetate, as the continuous phase in the first liquid, pairs wetting the inner tube wall, while kerosene, in the second liquid, pairs wetting the inner tube walls. The aquades-kerosene system could form a thin film but is not observed due to visual limitations. In many cases, particularly those involving mass and heat transfer, the film formation is more advantageous than flow patterns without films because the appearance of these films increases the interfacial mass/heat transfer rates. "*A*" is the surface area of the droplet where the mass/heat transfer happens, and "*V*" is the enclosed droplet volume. In a flow pattern without film, the mass/heat transfer process occurs in the zone between two droplets, between the heads and tails of successive droplets. However, in the flow pattern with film, a mass transfer does not only occur in that zone but also in the thin liquid film.

Effect of Inner Diameter of Microtube to Liquid-Liquid Flow Pattern

Two-phase flow patterns in aquades-kerosene and aquades-ethyl acetate with both dispersed and continuous phase flow rates of 25 ml/h in different tube diameters are shown in Fig. 6. The left figure is the flow pattern for aquades-kerosene, and the right one shows the flow pattern for aquades-ethyl acetate. Fig. 6 shows that a constant flow rate (25-25 ml/h) at various tube diameters formed the same flow pattern, slug flow. Thus, at a constant flow rate, the different tube diameter in this experiment does not affect the flow pattern type but rather the droplet length formed. At a specific flow rate, changes in tube diameter can cause changes in the type of flow pattern from slug flow to annular flow, mainly if a tube with a smaller diameter is used. From the droplets length measurement, in an aquades-kerosene system with a constant flow rate of 25-25 ml/h, the average length of droplets formed within a 0.5 mm diameter tube is 10.074 mm, tube diameter of 0.8 mm is 4.523 mm, and a tube with a diameter of 1 mm is 3,129 mm. At a constant flow rate, the tube diameter gets larger the shorter the droplet length. Further, from the observation, a thin liquid film appeared in the narrow space between the slug and the channel wall for aquades-ethyl acetate and without film for aquades-kerosene. The appearance of a thin liquid film certainly plays an important role in increasing the specific surface that can be generated by two-phase flow for mass/heat transfer processes.
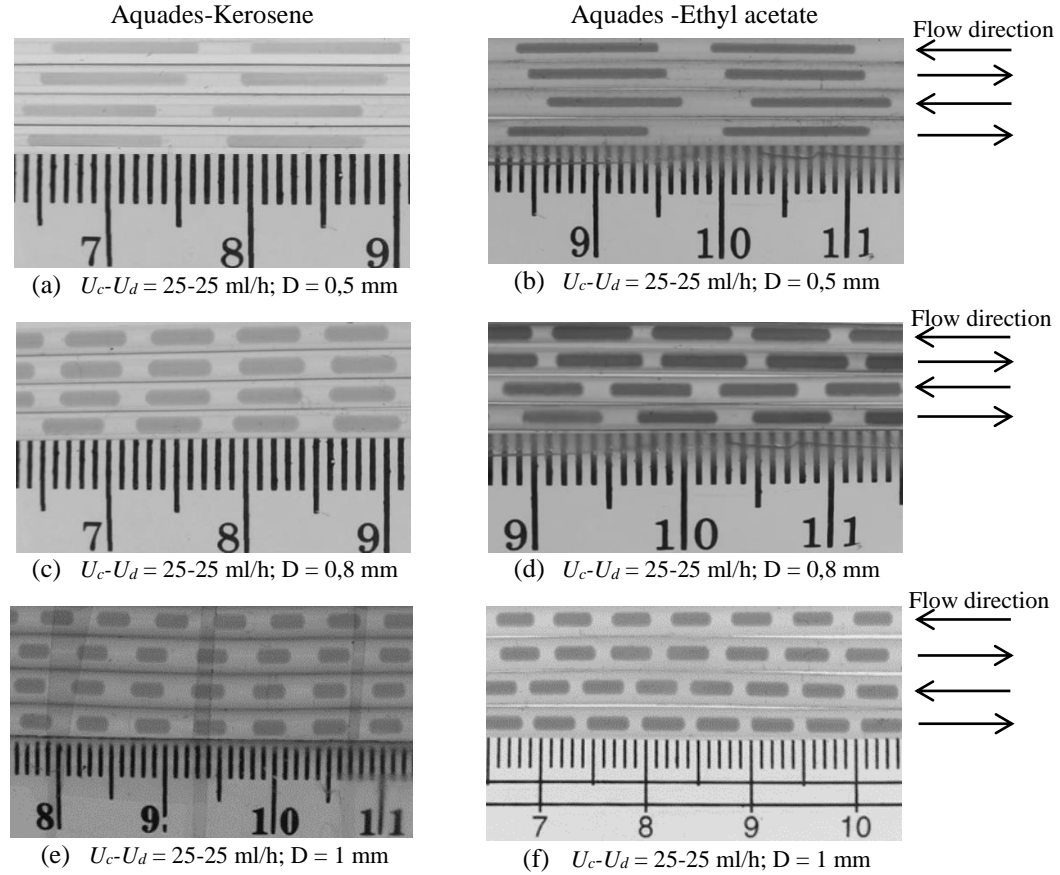
	Aquades-Kerosene		Aquades -Ethyl acetate
(a)	U_c-U_d = 25-25 ml/h; D = 0,5 mm	(b)	U_c-U_d = 25-25 ml/h; D = 0,5 mm
(c)	U_c-U_d = 25-25 ml/h; D = 0,8 mm	(d)	U_c-U_d = 25-25 ml/h; D = 0,8 mm
(e)	U_c-U_d = 25-25 ml/h; D = 1 mm	(f)	U_c-U_d = 25-25 ml/h; D = 1 mm

FIGURE 6. (a), (c), (e) Flow pattern in aquades-kerosene; (b), (d), (f) Flow pattern in aquades-ethyl acetate

The Stability of Slug Flow Pattern

The channel used in this observation was arranged into four rows. Fig. 7-9 shows the droplet profile within the microtube. The droplet length and distance were obtained by observing the flow pattern through an observation field with a 10 cm-long microtube. A computer program was used to measure the dimension of droplets.
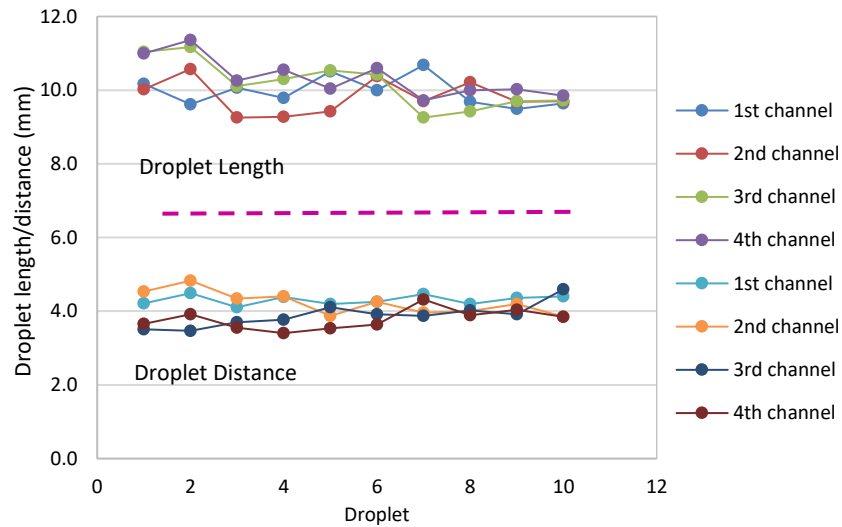

FIGURE 7. Droplet dimension profile in aquades-kerosene U_d-U_C = 25-25 ml/h (stable flow)
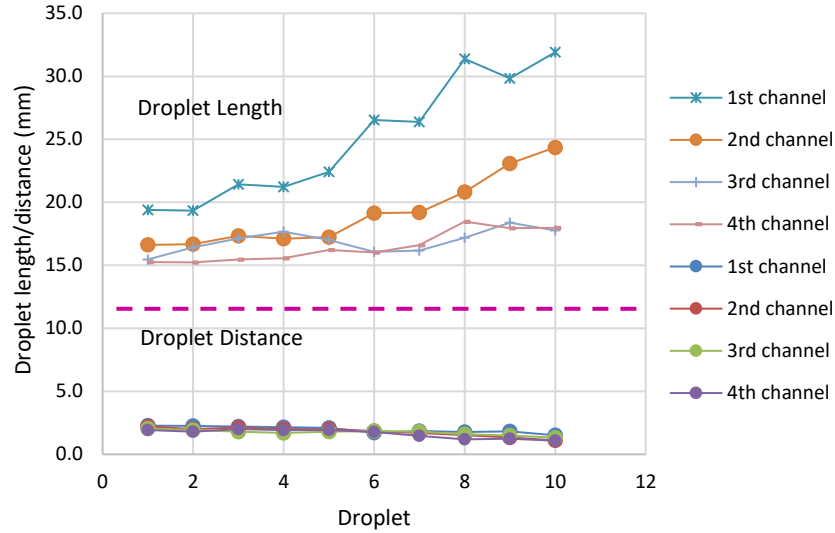
FIGURE 8. Droplet dimension profile in aquades-kerosene U_d-U_C = 35-25 ml/h (unstable flow)

Fig. 7 and 9 show a characteristic of stable flow, whereas Fig. 8 indicates an unstable flow pattern. A stable flow is defined as the flow with constant linear velocity and it has a regular and uniform shape and dimension of slug length. The droplets length and the distance of successive droplets in Fig. 7 and 9 are relatively similar, with a small deviation of less than 1 mm in length. On the contrary, Fig. 8 shows the higher deviation of these dimensions. The flow pattern in this figure has an unstable flow characteristic. The droplet length changed over time during observation, whereas the droplet distance was relatively constant.
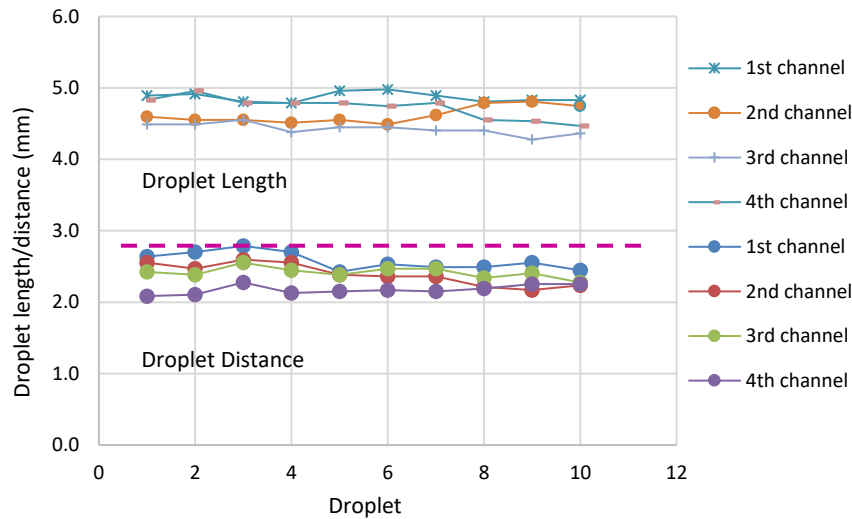

FIGURE 9. Droplet dimension profile in aquades-ethyl acetate U_d-U_C=70-70ml/h (stable flow)

The difference in droplet length, which is quite prominent in the microtube, is difficult to explain. This phenomenon may be caused by the pump's performance, which is unstable while pumping the two liquid phases, and another one is the coalescence phenomenon, mainly for tubes with huge length dimensions.

The stability of the slug flow formed in the microfluidic device is a goal that has always been realized. Due to the high flow stability in many heterogeneous systems applications, process behavior can be easily predicted and controlled. In heterogeneous systems involving mass/heat transfer, this mass/heat transfer process takes place through interfaces that appear around the slug, namely at the head, tail, and liquid film between the slug and the channel walls.

The Effect of the Linear Velocity Ratio of Dispersed to Continuous Phase (U_d/U_c) to Droplet Length (L_b)

TABLE 4. Effect of U_d/U_c to L_b in aquades-kerosene

Ud/Uc	Droplet Length			
	1st Channel	2nd Channel	3rd Channel	4th Channel
1	9.9638	9.8234	10.1681	10.3404
1.4	24.9872	19.1574	16.9298	16.4766
1.8	15.1936	15.6255	16.0043	16.3915
2.2	18.3106	18.1787	17.9872	18.9128

TABLE 5. Effect of U_d/U_c to L_b in aquades-ethyl acetate

U_d/U_c	Droplet Length			
	1st Channel	2nd Channel	3rd Channel	4th Channel
1	10.2000	9.7766	9.8170	9.8766
1.4	11.6957	11.6106	11.5447	12.0000
1.8	13.5787	12.7511	13.3340	12.8915
2.2	14.5957	13.5957	14.3617	14.3617

The larger U_d/U_c ratio was obtained by increasing the flow rate of aquades to the same flow rate of continuous phase increases in the droplet length dimensions in each microchannel. Table 4 indicates that an increase in two folds of the U_d/U_c ratio can increase the droplet length (L_b) by two times. The droplets on each microchannel show this tendency. However, the effect of increasing the U_d/U_c ratio differs from the results shown in Table 5, i.e., increasing the ratio up to 2 times can only increase 1.5 times the droplet length.

Bubble Length Follows Garstecky Model
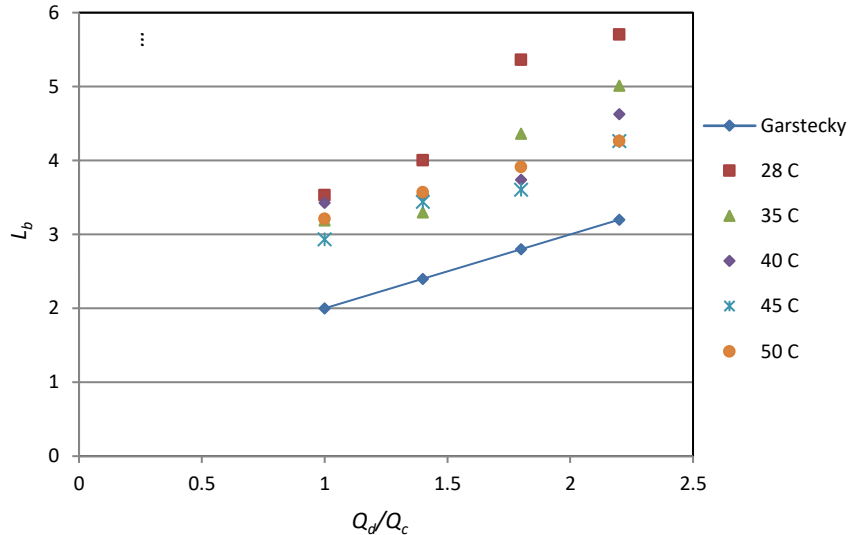

FIGURE 10. The comparison of the experimental droplets length and Garstecky model for the aquades-kerosene system, 1 mm inside diameter of the tube

The droplet length at the inlet section of the main channel has the dimension as shown in Fig. 10 and 11, Each for pairs of 2 liquid-liquid phases from aquades-kerosene and aquades-ethyl acetate. Garstecky, in the previous study, had

formulated the correlation between the length of droplets (L_b) formed in the T-junction on the various ratio of dispersed phase to continuous phase (Q_d/Q_c) following the equation as below: with Q_d = debit of the dispersed phase, Q_c = debit of the continuous phase, W_{in} = channel diameter in the inlet section of the dispersed phase (aquades), and W = diameter of the main channel.
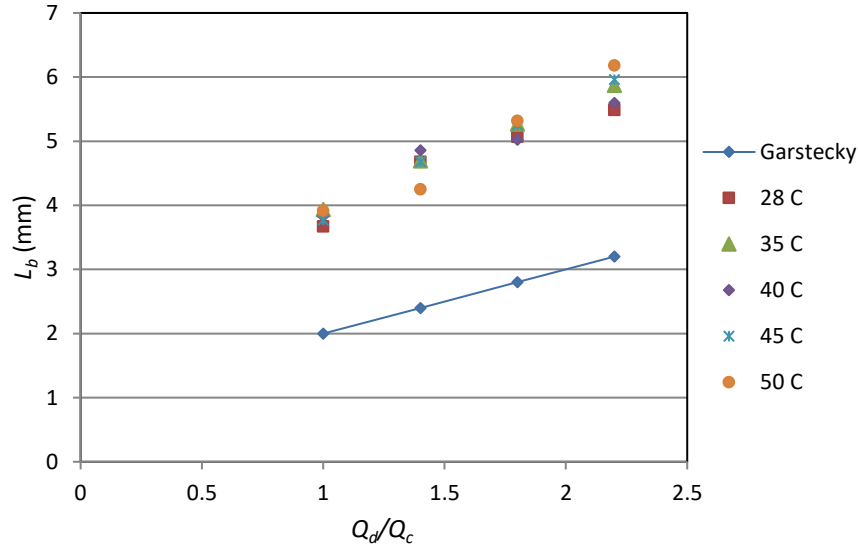

FIGURE 11. The comparison of the experimental droplets length and Garstecky model for the aquades-ethyl acetate system, 1 mm inside diameter of the tube

When compared, the length of the experimental droplet characteristic is appropriate to the proposed model by Garstecky. At the same time, the increase in Q_d/Q_c will be followed by the increase in the droplet length (L_b) with a linear trend. However, the values of L_b experiment and L_b based on this model were different. There are some possible factors: i.e., the Garstecky model has yet to consider the type of material channel, the liquid wettability to the inner wall of a microchannel, and the physical property such as liquid density and viscosity of the liquid that is used in the experiments.

Dimensionless Numbers

Capillary number, Reynold number, and Weber number are dimensionless numbers explaining the effect of three dominants force in a microchannel system: inertial force, viscous force, and surface tension force. By comparing these dimensionless numbers, the influence of dominant force or less dominant will be known in a slug flow formation of a liquid-liquid system. The capillary number represents the ratio of the following forces [10,11]:

$$Ca = \frac{viscous\,force}{surface\,tension\,force} \tag{1}$$

The capillary number in this experiment is $6.68 \times 10^{-5} - 8.719 \times 10^{-3}$ ($C_a < 1$). The value of capillary number below one indicates that surface tension force works more dominant than viscous force.
Reynold number represents the ratio of inertial forces to viscous force as in the following equation [11]:

$$Re = \frac{inertial\,force}{viscous\,force} \tag{2}$$

Reynold's number experiment is in the range of $3.2289 - 122.1798$ ($Re > 1$). The value of Reynold's number higher than one indicates that inertial force works more dominant than viscous force.
Weber number represents the ratio of inertial force to surface tension force as in the following equation [11]:

$$We = \frac{inertial\ force}{surface\ tension\ force} \qquad (3)$$

Weber's number in this experiment is $1.062 \times 10^{-3} - 1.841 \times 10^{-1} (We < 1)$. Weber's number below one indicates that surface tension is more dominant than inertial force. Based on the value of Capillary number, Reynold number, and Weber number, the influence of these forces on the liquid-liquid system of aquades-kerosene and aquades-ethyl acetate has the following order: surface tension force > inertial force > viscous force. The effect of inertial force increases with an increasing linear velocity of ρU^2 (U = linear velocity of liquid). Specifically, at the higher linear velocity of the continuous phase on the constant velocity of the dispersed phase, the slugs that appeared in the channel have a smaller dimension, and vice versa at a constant velocity of the continuous phase on a higher velocity of the dispersed phase, the slugs in the channel have a longer dimension. If the ratio of the linear velocity of the dispersed to the continuous phase continuously increases, the flow pattern formed will transform into an annular type. Further, besides inertial forces, an increase in liquid velocity also increased the effect of viscous force on liquid-liquid systems with a linear correlation at a specific viscosity, $\mu U/l$ (μ = viscosity, l = length). Knowing the dominant forces working on each phase will make it easier to determine the discharge ratio of the dispersed and continuous phases to produce the slug flow pattern of the liquid mixture used.

CONCLUSION

The slug flow hydrodynamic was investigated in a circular silicone microchannel with an inside diameter of less than 1 mm. The tube diameter in these experiments (0.5, 0.8, 1 mm) did not affect the flow pattern type; it affected the droplet length and the distance of successive droplets. The increased channel diameter has brought on the lower droplet length. The slug flow pattern formed when the flow velocity ratio of the dispersed to continuous phase (U_d/U_c) = 1; 1,4; 1,8; 2,2. The greater value of U_d/U_c has resulted in the length of droplets within the microchannel. The various flow velocity used in these experiments consist of U_c = 25; 70 ml/h, U_d = 25; 35; 45; 55; 70 ml/h, entirely formed slug flow pattern.

The higher temperature may influence the droplet lengths and the distances of successive droplets. The temperature correlates with the viscosity of the liquid-liquid two-phase flow. Further, the droplet length showed the same trend as the length obtained by the Garstecky model.

The dimensionless numbers consisting of the Capillary Number, Reynold Number, and Weber Number can explain the influence of three dominant forces in a microsystem, i.e., surface tension, inertial, and viscous force.

REFERENCES

1. R. Antony, M. S. Giri Nandagopal, N. Sreekumar, S. Rangabhashiyam, and N. Selvaraju, Bulletin of Chemical Reaction Engineering & amp;Amp; Catalysis **9**, 207 (2014).
2. R. K. Verma and S. Ghosh, Chemical Engineering Journal **397**, 125443 (2020).
3. Q. Zhang, H. Liu, S. Zhao, C. Yao, and G. Chen, Chemical Engineering Journal **358**, 794 (2019).
4. A. V. Kovalev, A. A. Yagodnitsyna, and A. V. Bilsky, Chem Eng Technol **44**, 365 (2021).
5. L. Lei, Y. Zhao, W. Chen, H. Li, X. Wang, and J. Zhang, 1 (2021).
6. W. Zhou, E. V Rebrov, and T. A. Nijhuis, **66**, 42 (2011).
7. B. Sunden, Slug formation Analysis of Liquid-liquid Two-Phase Flow in T-junction Microchannel, **11**, 1 (2019).
8. A. V Kovalev, A. A. Yagodnitsyna, and A. V Bilsky, Chemical Engineering Journal **352**, 120 (2018).
9. "A comprehensive review on liquid-liquid two-phase flow.pdf
10. N. Volkel, A. Y. Widianto, J. Aubin, and C. Xuereb, *Gas-Liquid Taylor Flow Characteristics in Straight and Meandering Rectangular Microchannels* (2008).
11. V. Talimi, Y. S. Muzychka, and S. Kocabiyik, International Journal of Multiphase Flow **39**, 88 (2012).

AIP Conference Proceedings

International Seminar on Chemical Engineering Soehadi Reksowardojo (STKSR) 2022

Ambon, Indonesia • 9–10 August 2022

Editors • Jenny Rizkiana, Khoiruddin Khoiruddin, Kiki Adi Kurnia, Aqsha Aqsha and Helen Julian

STKSR 2022
Ambon, Indonesia

Internasional Seminar on Chemical Engineering
Soehadi Reksowardojo (STKSR) 2022

Available Online: pubs.aip.org/aip/acp

Issues

Select Decade 2020 ⌄

Select Year 2024 ⌄

Issue 7 March - Volume 3073, Issue 1 ⌄

PRELIMINARY

Preface: International Seminar on Chemical Engineering Soehadi Reksowardojo (STKSR) 2022 🛒
AIP Conf. Proc. 3073, 010001 (2024) https://doi.org/10.1063/12.0024178

View article   🄿 PDF

BIOENERGY AND ALTERNATIVE ENERGY

Synthesis of gel polymer electrolyte (GPE) with redox active addition for supercapacitor applications based on activated carbon electrode from OPEFB 🛒

Tiara Ariani Putri; Heri Rustamaji; Hary Devianto; Tirto Prakoso;
Pramujo Widiatmoko

AIP Conf. Proc. 3073, 020001 (2024) https://doi.org/10.1063/5.0194298

Abstract ⌄   View article   🄿 PDF

Dye sensitized solar cell performance analysis through

Review article: Application of integrated electrodes materials for enhancing the electrochemical reduction of carbon dioxide 🛒

Hary Devianto; Mitra Eviani; Tirto Prakoso

AIP Conf. Proc. 3073, 020003 (2024) https://doi.org/10.1063/5.0194297

Abstract ⌄   View article   📄 PDF

Analysis of the behavior of ionic conductivity in alkaline hydrogel polymer electrolytes to improve of the performance aspect of zinc-air batteries 🛒

Hary Devianto; Tirto Prakoso; Pramujo Widiatmoko; Pramahadi Febriyanto; Mohammad Ghimnastiar Ulsak

AIP Conf. Proc. 3073, 020004 (2024) https://doi.org/10.1063/5.0194295

Abstract ⌄   View article   📄 PDF

Carbon credit and economic feasibility analysis of biomass-solar PV-battery power plant for application in Nusa Penida - Bali 🛒

Dindamilenia Choirunnisa Hardiyasanti; Sinta Widianingrum; Aditiya Harjon Bahar; Djati Wibowo Djamari; Jaya Wahono

AIP Conf. Proc. 3073, 020005 (2024) https://doi.org/10.1063/5.0194351

Abstract ⌄   View article   📄 PDF

Interaction of biomass and biochar of seaweed and apple tree branch in two-stage co-gasification system 🛒

Yohanes Andre Situmorang; Guoqing Guan

AIP Conf. Proc. 3073, 020006 (2024) https://doi.org/10.1063/5.0195000

Abstract ⌄   View article   📄 PDF

Simulation of alkali metals behavior and ash fusion in empty fruit bunch and palm kernel shell combustion using thermodynamic model 🛒

Winny Wulandari; Raihan Raihan; Muhammad Syaiful Islam; Tjokorde Walmiki Samadhi

AIP Conf. Proc. 3073, 020008 (2024) https://doi.org/10.1063/5.0193708

Abstract ⌄   View article   🅟 PDF

Opportunities and challenges in utilizing palm kernel shell as renewable energy source in ceramic tile production 🛒

Handaya Handaya; Charlie Dhiannova; Herri Susanto

AIP Conf. Proc. 3073, 020009 (2024) https://doi.org/10.1063/5.0194839

Abstract ⌄   View article   🅟 PDF

Masaro incinerator for non biodegradable and non recycled waste handling at Babakan village, Ciwaringin district, Cirebon 🛒

A. Z. Abidin; M. I. Maulana; A. Aqsha; T. Abidin

AIP Conf. Proc. 3073, 020010 (2024) https://doi.org/10.1063/5.0199437

Abstract ⌄   View article   🅟 PDF

Utilization of water hyacinth as biomass fuel pellet: Small and medium enterprise approach 🛒

Maria Gabriela Kristanti; Herri Susanto

AIP Conf. Proc. 3073, 020011 (2024) https://doi.org/10.1063/5.0199208

Abstract ⌄   View article   🅟 PDF

    Abstract ⌄   View article   🗎 PDF

Process modeling of hydrogen energy production from biomass through steam reforming method and optimization using response surface methodology 🛒

Muhammad Ikhsan Taipabu; Wei Wu; Karthickeyan Viswanathana;
Nikmans Hattu; Ervina Rumpakwakra

AIP Conf. Proc. 3073, 020013 (2024) https://doi.org/10.1063/5.0199204

    Abstract ⌄   View article   🗎 PDF

The thermal characteristics of lithium-ferro-phosphate (LFP) battery pack 🛒

Arthanta Cracian; Umar Said; Sugeng Winardi; Suci Madhania

AIP Conf. Proc. 3073, 020014 (2024) https://doi.org/10.1063/5.0193636

    Abstract ⌄   View article   🗎 PDF

DC pump performance testing using solar power 🛒

J. J. S. Dethan; F. J. Haba Bunga; M. L. Lano; M. Makaborang; N. P. P. E. Nainiti; Hary Devianto

AIP Conf. Proc. 3073, 020015 (2024) https://doi.org/10.1063/5.0193716

    Abstract ⌄   View article   🗎 PDF

FOOD ENGINEERING AND TECHNOLOGY

Preliminary study: Acid effect in the improvement of extraction yield and antioxidant activity in tomato 🛒

Angela Justina Kumalaputri; Angela Rianti; Gracia Alfaviona Limiarto;

Abstract ⌄   View article   🗋 PDF

Comparative analysis of the proximate content, free phenolics, bound phenolics, and total phenolics of defatted and non-defatted rice bran 🛒

Zahara Mardiah;   Soen Steven;   Dian Shofinita;   Johnner Sitompul

Abstract ⌄   View article   🗋 PDF

Integrated wet process for coconut protein and VCO production 🛒

Dianika Lestari;   Anisa Auvira;   Rahmaniah Akhirunnisa

Abstract ⌄   View article   🗋 PDF

Ultrasonic-assisted extraction optimization of the flavonoid compounds from Vernonia amygdalina Del. leaves using response surface method 🛒

B. Buanasari;   Danu Ariono;   Johnner P. Sitompul

Abstract ⌄   View article   🗋 PDF

Pectin extraction from apple pomace (*Malus domestica*) as gelatin replacer using living cells with ultrasound pretreatment 🛒

Nurul Rahmawati;   Orchidea Rachmaniah;   Tri Widjaja;   Setiyo Gunawan

Abstract ⌄   View article   🗋 PDF

Comparative chemical profiles of essential oil of nutmeg flesh (*Myristica fragrans* Houtt) through multiple drying methods 🛒

Sophia Grace Sipahelut; Ivonne Telussa

Abstract ⌄   View article   🗋 PDF

Growth and carrageenan content of red algae, *Kappahycus alvarezii* (doty) doty different varieties farming using different methods and different habitats in Bolok waters, Kupang Regency 🛒

Wilson L. Tisera; Hildegardus Asa; Lienda A. Handojo; Rockie R. L. Supit; Alfred G. O. Kase; Donny M. Bessie; Dewi Setiyowati Gadi; Ima D. Saleky; Vania R. T. Tisera

Abstract ⌄   View article   🗋 PDF

Traditional salt production from improved cooking tools in the tiberias community, West Oesapa village, city of Kupang 🛒

Umbu Paru Lowu Dawa; Mada Mariana Lakapu; Dewi Setyowati Gadi; Yunialdi H. Teffu; Dewanto Umbu Saga Anakaka; Fanny Iriany Ginzel; Sanggono Adisasmito

Abstract ⌄   View article   🗋 PDF

Composition of pigments in brown algae collected from Bolok marine waters 🛒

Alfred G. O. Kase; Yohanes Merryanto; Wilson Tisera; Donny M. Bessie; Rockie R. L. Supit; Dionisius A. Samsop; Beatrix M. Rehatta; Cristiani Soi Meo; Umbu Paru Lowu Dawa; Ayub U. I. Meko; Lienda A. Handojo

AIP Conf. Proc. 3073, 030012 (2024) https://doi.org/10.1063/5.0194092

Abstract ⌄   View article   🗎 PDF

Analysis of bacteria caused ice-ice disease in seaweed through polyculture in Dengka Island, Rote Ndao Regency 🛒

Donny M. Bessie; Wilson L. Tisera; Umbu P. L. Dawa; Alfred G. O. Kase; Vania R. T. Tisera; Nina J. Lapinangga; Sanggono Adisasmito

AIP Conf. Proc. 3073, 030013 (2024) https://doi.org/10.1063/5.0193767

Abstract ⌄   View article   🗎 PDF

Effects of tongka langit banana (*Musa troglodytarum*) puree concentrations on the quality of Yoghurt 🛒

Lorina Sahetapy; Helen Cynthia Dewi Tuhumury; Erynola Moniharapon

AIP Conf. Proc. 3073, 030014 (2024) https://doi.org/10.1063/5.0193876

Abstract ⌄   View article   🗎 PDF

Effect of vacuum pressure on drying of durian fruit (*Durio zibethinus*) 🛒

Sanggono Adisasmito; Lienda Aliwarga; Farah Hafizhah

AIP Conf. Proc. 3073, 030015 (2024) https://doi.org/10.1063/5.0193635

Abstract ⌄   View article   🗎 PDF

BIOPROCESS ENGINEERING

Antibacterial activity of copper nanoparticles (CuNPs) by chemical reduction method 🛒

Rosi Wulandari; Yuni Kusumastuti; Agus Prasetya; Yekti Asih Purwestri; Himawan T. B. M. Petrus; Arifudin Idrus; Masaru Tanaka

AIP Conf. Proc. 3073, 040001 (2024) https://doi.org/10.1063/5.0193978

Abstract ⌄   View article   🅿 PDF

Preliminary study of biological route of vanilin production from palm oil empty fruit bunch (EFB) delignification liquor 🛒

Syahdan A. Muhammad; M.T.A.P. Kresnowati

AIP Conf. Proc. 3073, 040002 (2024) https://doi.org/10.1063/5.0196016

Abstract ⌄   View article   🅿 PDF

Isolation and screening of actinomycetes active against plant pathogenic fungi 🛒

Rofiq Sunaryanto; Yusriani Sapta Dewi; Nurhayati Nurhayati; Johnner Sitompul

AIP Conf. Proc. 3073, 040003 (2024) https://doi.org/10.1063/5.0194400

Abstract ⌄   View article   🅿 PDF

CHEMURGY AND BIO-BASED MATERIALS

Hydrothermal carbonization of de-ashed seaweed in the

Perspective through Monte Carlo simulations for open field burning emission in Indonesia and alternative way of using rice straw as particle board production 🛒

Mekro Permana Pinem; Yusvardi Yusuf; Dhimas Satria; Shofiatul Ula; Dwiananto Sukamto; Agung Sudrajat; Kurniawan Putra Yudha

AIP Conf. Proc. 3073, 050002 (2024) https://doi.org/10.1063/5.0193647

Abstract ⌄   View article   🗎 PDF

Chitosan-polyvinyl alcohol (PVA) based composite biofilm: The effect of solvent and nanofiller 🛒

Bintang Junita Siom; Jayanudin; Mekro Permana Pinem; Endarto Yudo Wardhono

AIP Conf. Proc. 3073, 050003 (2024) https://doi.org/10.1063/5.0194406

Abstract ⌄   View article   🗎 PDF

Analysis and characterization of microcrystalline cellulose synthesized from microwave-assisted hydrolysis of sugarcane bagasse 🛒

A. S. R. B. Latifa; W. B. Sediawan; M. Fahrurrozi

AIP Conf. Proc. 3073, 050004 (2024) https://doi.org/10.1063/5.0201506

Abstract ⌄   View article   🗎 PDF

Synthesis of activated carbon from bamboo biomass for supercapacitor electrodes with various types of electrolytes 🛒

Fena Retyo Titani; Heri Rustamaji; Tirto Prakoso; Hary Devianto; Pramujo Widiatmoko; Astri Nur Istyami

AIP Conf. Proc. 3073, 050005 (2024) https://doi.org/10.1063/5.0194255

Abstract ⌄   View article   🗎 PDF

Overview of torrefaction technology for promotion palm oil solid waste to energy biochar 🛒

Asri Gani; Erdiwansyah; Edi Munawar; Muhammad Faisal; Mahidin; Muhammad Zaki; Muhammad Nizar

AIP Conf. Proc. 3073, 050007 (2024) https://doi.org/10.1063/5.0194128

| Abstract ∨ | View article | 🗎 PDF |

Synthesis and thermal stabilizing effect on polyvinyl chloride of calcium/zinc carboxylate from palm fatty acid distillate: Effect of metal to fatty acid ratio 🛒

I. Dewa Gede Arsa Putrawan; Nadya Amalia Pratiwi Nento; Adli Azharuddin; Antonius Indarto; Dendy Adityawarman

AIP Conf. Proc. 3073, 050008 (2024) https://doi.org/10.1063/5.0193942

| Abstract ∨ | View article | 🗎 PDF |

Biodegradable foam production process based on extracted cellulose of empty palm oil fruit bunch and chitosan for food packaging 🛒

Ihza Aulia Alfarisi; Havid Arga Kusumamurti; Fuad Dimar Fauzi; Yunita Aprilia; Muhammad Luqman Qodarusman; Sunu Herwi Pranolo

AIP Conf. Proc. 3073, 050009 (2024) https://doi.org/10.1063/5.0193629

| Abstract ∨ | View article | 🗎 PDF |

Implementation of MASARO technology for compostable waste processing at Institut Teknologi Bandung – Jatinangor campus 🛒

A. Z. Abidin; H. P. R. Graha; E. V. Yemensia; H. M. Anzhari; M. I. Maulana

Abstract ∨   View article   ⬙ PDF

Adding adhesive on making of waste bricket of eucalyptus oil refining 🛒

Arlindo Umbu S. Kette; Jimmy J. S. Dethan; Fredrik J. Haba Bunga;
Nohyanto Banfatin; Ronny Purwadi

Abstract ∨   View article   ⬙ PDF

Preliminary study on palm kernelamidopropyl betaine (PKAPB) production route 🛒

Astri Nur Istyami; Amanda Nazwa Nur Fatihah; Meiti Pratiwi; Ronny
Purwadi; Dianika Lestari

Abstract ∨   View article   ⬙ PDF

Synthesis of hydrochar from empty fruit bunches (EFB) and oil palm trunks (OPT) *Via* wet torrefaction: A parametric study 🔓

Frederick Jit Fook Phang; Megan Soh; Jiuan Jing Chew; Aqsha Aqsha;
Deni Shidqi Khaerudini; Gerald Ensang Timuda; Bing Shen How; Soh
Kheang Loh; Suzana Yusup; Jaka Sunarso

Abstract ∨   View article   ⬙ PDF

Lignocellulosic biomass fractionation through biphasic-solvent system 🛒

Characteristics of kesambi leaf torrefaction biomass 🛒

Jemmy J. S. Dethan; Jublin F. Bale-Therik; Franky M. S. Telupere; Herianus J. D. Lalel; Sanggono Adisasmito

AIP Conf. Proc. 3073, 050016 (2024) https://doi.org/10.1063/5.0193717

Abstract ∨   View article   🗎 PDF

ADVANCED SCIENCE AND MATERIALS

Ionic liquid-based electrolyte in supercapacitors 🛒

Viona Aulia Rahmi; Megawati Zunita

AIP Conf. Proc. 3073, 060001 (2024) https://doi.org/10.1063/5.0193936

Abstract ∨   View article   🗎 PDF

Optimization of banten ilmenite leaching using hydrochloric acid 🛒

Venisa Mega Puteri Anggraeni; Chandra Wahyu Purnomo; Himawan Bayu Tri Murti Petrus

AIP Conf. Proc. 3073, 060002 (2024) https://doi.org/10.1063/5.0200301

Abstract ∨   View article   🗎 PDF

The characterization and electrochemical properties of copper-complex 🛒

Kariana Kusuma Dewi; Ni Luh Wulan Septiani; Muhammad Iqbal; Nugraha Nugraha; Brian Yuliarto

AIP Conf. Proc. 3073, 060003 (2024) https://doi.org/10.1063/5.0199392

Abstract ∨   View article   🗎 PDF

Fabrication and performance of nickel-cobalt hydrogen phosphate-based supercapacitor 🛒

Wulan Kusuma Wardani; Ni Luh Wulan Septiani; Ahmad Nuruddin; Muhammad Iqbal; Nugraha Nugraha; Brian Yuliarto

AIP Conf. Proc. 3073, 060005 (2024) https://doi.org/10.1063/5.0199394

Abstract ∨   View article   🗋 PDF

Zeolitic imidazolate framework 8 (ZIF-8) as sensing material for electrochemical detection of dopamine 🛒

Nurul Hanifah; Ni Luh Wulan Septiani; Nugraha Nugraha; Siti Nurul Aisyiyah Jenie; Brian Yuliarto

AIP Conf. Proc. 3073, 060006 (2024) https://doi.org/10.1063/5.0199393

Abstract ∨   View article   🗋 PDF

Preliminary design precipitated calcium carbonate from blast furnace gas and steel slag plant 🛒

Kusdianto Kusdianto; Nurdiana Ratna Puri; Arthanta Cracian; Umar Said; Suci Madhania; Siti Machmudah; Sugeng Winardi

AIP Conf. Proc. 3073, 060007 (2024) https://doi.org/10.1063/5.0195561

Abstract ∨   View article   🗋 PDF

Dynamic of microemulsion nanoparticle precipitation: Sensitivity analysis of particle nucleation and growth order 🛒

Dendy Adityawarman; Sumriamin Rambe

AIP Conf. Proc. 3073, 060008 (2024) https://doi.org/10.1063/5.0195823

Abstract ∨   View article   🗋 PDF

Identifying microplastic particle in the drinking water using Raman spectroscopy method 🛒

Akhmad Zainal Abidin; Elsye Veradika Yemensia; Hafis Pratama Rendra Graha; Hadi Mulya Anshari

AIP Conf. Proc. 3073, 060010 (2024) https://doi.org/10.1063/5.0199439

Abstract ⌄   View article   🗎 PDF

Potential research of study PVC products life cycle assessment in Indonesia 🛒

Ernie S. A. Soekotjo; Andro Alfiandi; Elsye Veradika Yemensia; Nugroho Adi Sasongko; Hafis Pratama Rendra Graha; Akhmad Zainal Abidin

AIP Conf. Proc. 3073, 060011 (2024) https://doi.org/10.1063/5.0199436

Abstract ⌄   View article   🗎 PDF

On the influence of silica nanoparticles for enhanced oil recovery (EOR) 🛒

Sarah Dampang; Muhammad Mufti Azis; Ahmad Tawfiequrrahman Yuliansyah; Suryo Purwono

AIP Conf. Proc. 3073, 060012 (2024) https://doi.org/10.1063/5.0194108

Abstract ⌄   View article   🗎 PDF

Antibacterial properties of graphene-based nanomaterials and graphene-based nanocomposites: A mini review 🛒

Vita Wonoputri; Hans Vito Xavier Khosasih; Robby Lysander Aurelio

AIP Conf. Proc. 3073, 060013 (2024) https://doi.org/10.1063/5.0194495

Abstract ⌄   View article   🗎 PDF

Parameters influencing stable colloidal ZnO from zinc acetate dihydrate using sol-gel method 🛒

Nurdiana Ratna Puri; Fatiya Rizkiyani; Fakhri Jayadi; Lailatul Qomariyah; Kusdianto Kusdianto; Sugeng Winardi

AIP Conf. Proc. 3073, 060015 (2024) https://doi.org/10.1063/5.0195406

Abstract ∨	View article	🗎 PDF

Determination of corrosion & mitigation on stainless steel 22 cr using weight thickness method in production in a corrosion environment 🛒

A. A. Pramana; R. F. Yusuf

AIP Conf. Proc. 3073, 060016 (2024) https://doi.org/10.1063/5.0193648

Abstract ∨	View article	🗎 PDF

SEPARATION TECHNOLOGY

Study on microfiltration of crude biodiesel using ceramic membrane 🛒

Samuel P. Kusumocahyo; Natasya Z. Az'zura; Silvya Yusri; Hery Sutanto; Meliyanti Meliyanti; Eneng Maryani; Hernawan Hernawan

AIP Conf. Proc. 3073, 070001 (2024) https://doi.org/10.1063/5.0194863

Abstract ∨	View article	🗎 PDF

Polyethylene terephthalate ultrafiltration membrane for separation and purification process of coffee pulp extract solution 🛒

Samuel P. Kusumocahyo; Silvya Yusri; Diah I. Widiputri; Febbyandi I. Pandiangan; Rizal P. Ramdhani

AIP Conf. Proc. 3073, 070002 (2024) https://doi.org/10.1063/5.0194864

Abstract ∨   View article   📄 PDF

Techno-economic analysis of coal leaching processes to produce ultra clean coal 🛒

Abdul Rahman Marwis Karim; Indah Nurani; Tiva Putri Tri Lestari; Joko Wintoko; Muhammad Mufti Azis

AIP Conf. Proc. 3073, 070004 (2024) https://doi.org/10.1063/5.0194853

Abstract ∨   View article   📄 PDF

Preparation and characterization of the improved-hydrophilic polyvinylidene fluoride (PVDF) membrane modified by polymer blending technique 🛒

Muhfadzallah Muhfadzallah; Sri Aprilia; Syawaliah Muchtar; Mukramah Yusuf; Umi Fathanah

AIP Conf. Proc. 3073, 070005 (2024) https://doi.org/10.1063/5.0194157

Abstract ∨   View article   📄 PDF

Removal of acrylic acid-containing industrial wastewater by coagulation, flocculation, and adsorption in a mini pilot scale 🛒

Johnner Sitompul; Jonathan Sangwha Lee; Yusriani Sapta Dewi; Tifari Athia Zahra

AIP Conf. Proc. 3073, 070006 (2024) https://doi.org/10.1063/5.0200087

Abstract ∨   View article   📄 PDF

Kinetics and isotherm adsorption models of acid mine drainage heavy metal using modified clay 🛒

Elvi Restiawaty; Wibawa Hendra Saputera; Qiston Naufal Javirian; Elicia Kusuma

Determination of the mobile phase in low-pressure column chromatography using thin-layer chromatography to purify astaxanthin ⛫

Putri Restu Dewati; Rochmadi Rochmadi; Abdul Rohman; Darwito Darwito; Arief Budiman

AIP Conf. Proc. 3073, 070008 (2024) https://doi.org/10.1063/5.0194483

| Abstract ⌄ | View article | ⬇ PDF |

Organic fouling mechanism in ultrafiltration membrane for drinking water ⛫

Anita Kusuma Wardani

AIP Conf. Proc. 3073, 070009 (2024) https://doi.org/10.1063/5.0193627

| Abstract ⌄ | View article | ⬇ PDF |

Evaluation of osmotic pressured membrane performance in achieving water sustainability ⛫

Jeremiah Tjandra; Natasya Angelina; Danu Ariono; Graecia Lugito

AIP Conf. Proc. 3073, 070010 (2024) https://doi.org/10.1063/5.0193853

| Abstract ⌄ | View article | ⬇ PDF |

Techno-economic analysis of caustic soda production in Indonesia based on membrane technology ⛫

Rendra Panca Anugraha; Juwari Juwari; Renanto Renanto; Sahara Putri Fachrudya; Yuliana Erika Daoed

AIP Conf. Proc. 3073, 070011 (2024) https://doi.org/10.1063/5.0193630

| Abstract ⌄ | View article | ⬇ PDF |

Crystallization of potassium chloride from its solution

Adsorption kinetics of amoxicillin, ampicillin, and doripenem on organobentonite 🔓

Jason Yi Juang Yeo; Aqsha Aqsha; Suryadi Ismadji; Jaka Sunarso

AIP Conf. Proc. 3073, 070013 (2024) https://doi.org/10.1063/5.0194120

Abstract ⌄   View article   🗎 PDF

PROCESS SIMULATION

Comparing options of BECCS in Indonesia using energy system modelling 🛒

Anggit Raksajati; Zefania P. Sutrisno; Attaya A. Meiritza

AIP Conf. Proc. 3073, 080001 (2024) https://doi.org/10.1063/5.0194372

Abstract ⌄   View article   🗎 PDF

Captured three-dimensional turbulent behaviors inside cyclones using computational fluid dynamics (CFD) design method 🛒

Soen Steven; Pandit Hernowo; Imam Mardhatillah Fajri; Pasymi Pasymi; Elvi Restiawaty; Yazid Bindar

AIP Conf. Proc. 3073, 080002 (2024) https://doi.org/10.1063/5.0199443

Abstract ⌄   View article   🗎 PDF

Improved operational unit process performance through three-dimensional design modifications using computational fluid dynamics method 🛒

Yazid Bindar; Soen Steven; Pandit Hernowo; Pasymi Pasymi; Elvi Restiawaty

AIP Conf. Proc. 3073, 080003 (2024) https://doi.org/10.1063/5.0199444

Abstract ⌄   View article   🅟 PDF

Simplified simulation of glucose hydrolysis to levulinic acid for estimating kinetic parameters 🛒

Meutia Ermina Toif; Savitri Kamila Fatma; Muslikhin Hidayat; Rochmadi Rochmadi; Arief Budiman

AIP Conf. Proc. 3073, 080005 (2024) https://doi.org/10.1063/5.0194484

Abstract ⌄   View article   🅟 PDF

Simulation of photocatalytic degradation of methylene blue using titanium dioxide (TiO$_2$) P25 as a photocatalyst 🛒

Wibawa Hendra Saputera; Dwiwahju Sasongko; Pramujo Widiatmoko; Nitya Yatasha Dewi; Awanis Mazayasina Ardhistira

AIP Conf. Proc. 3073, 080006 (2024) https://doi.org/10.1063/5.0194112

Abstract ⌄   View article   🅟 PDF

Heat transfer coefficient on stirring palm fatty acid distillate in a jacketed tank at a dynamic stage 🛒

I. Dewa Gede Arsa Putrawan; Yona Octavia; Adli Azharuddin; Antonius Indarto; Dendy Adityawarman

AIP Conf. Proc. 3073, 080007 (2024) https://doi.org/10.1063/5.0193948

Abstract ⌄   View article   🅟 PDF

Simulation study on commercial polypropylene production - Effect of productivity on the required reactor coolant and catalyst 🛒

Tri Partono Adhi; Dodi Afandi

AIP Conf. Proc. 3073, 080008 (2024) https://doi.org/10.1063/5.0194737

Abstract ⌄   View article   🅟 PDF

Analysis of changes in gas turbine compressor operation in gas processing station from parallel to series using aspen hysys 🛒

Patria Suryatmaja;   Hafid Alwan;   Indar Kustiningsih;   Yazid Bindar

AIP Conf. Proc. 3073, 080010 (2024) https://doi.org/10.1063/5.0199671

Abstract ⌄   View article   🅟 PDF

Techno-economic study of optimized multi-stage flash vaporization based condensate stabilization unit 🛒

Tri Partono Adhi;   Hilman Ali Hazmi

AIP Conf. Proc. 3073, 080011 (2024) https://doi.org/10.1063/5.0194740

Abstract ⌄   View article   🅟 PDF

INDUSTRIAL APPLICATION

Chemical looping coal gasification for IGCC process feed 🛒

Jenny Rizkiana;   Muhammad Ariqsyah Indra;   Hans Adrian;   Dwiwahju Sasongko;   Agus Tendi Ahmad Bustomi

AIP Conf. Proc. 3073, 090001 (2024) https://doi.org/10.1063/5.0193633

Abstract ⌄   View article   🅟 PDF

Determination of the effect of elevation on internal corrosion and mitigation in Cs pipeline using Olga simulator 🛒

Review electrochemical reduction of carbon dioxide into formic acid in various reactors using carbon-based catalyst 🛒

N. D. Jayanti;   H. Devianto;   P. Widiatmoko;   T. Prakoso;   M. Eviani

AIP Conf. Proc. 3073, 100001 (2024) https://doi.org/10.1063/5.0194299

Abstract ⌄   View article   🄳 PDF

Carbon capture and storage to simultaneous biogas purification and precipitated calcium carbonate production using Ca(OH)$_2$ aqueous solution in a bubble column reactor 🛒

Suci Madhania;   Muhammad Hubbal;   Faris Virgiansyah;   M. Fauzan Firdaus;   Kusdianto Kusdianto;   Siti Machmudah;   Sugeng Winardi

AIP Conf. Proc. 3073, 100002 (2024) https://doi.org/10.1063/5.0195403

Abstract ⌄   View article   🄳 PDF

Instability identification of three-bed Haber-Bosch ammonia synthesis process 🛒

Avariz Muhammad;   Tri P. Adhi

AIP Conf. Proc. 3073, 100003 (2024) https://doi.org/10.1063/5.0193812

Abstract ⌄   View article   🄳 PDF

Catalytic hydrogenolysis of glycerol to produce monoalcohols 🛒

Eka M. Idzati;   Firman Kurniawansyah;   Hikmatun Ni'mah;   Mahfud Mahfud;   Tantular Nurtono;   Achmad Roesyadi

AIP Conf. Proc. 3073, 100004 (2024) https://doi.org/10.1063/5.0194429

Abstract ⌄   View article   🄳 PDF

Investigation of nickel-impregnated niobium oxide catalyst to improve the quality of low-grade polyethylene pyrolysis oils composition via catalytic reforming 🛒

Fahrizal Nasution; Husni Husin; Mahidin Mahidin; Faisal Abnisa;
Komala Pontas; Ahmadi Ahmadi

AIP Conf. Proc. 3073, 100006 (2024) https://doi.org/10.1063/5.0193884

Abstract ∨	View article	🗎 PDF

Initial approach of Nbopo$_4$ ability to hydrodeoxygenation reaction of palm oil based on ATR-IR spectra alteration 🛒

Firda Tirta Yani; Husni Husin; Darmadi Darmadi; Syaifullah Muhammad;
Mukhlishien Mukhlishien; Suraiya Kamaruzzaman; Harrin Fajrin Alfiar

AIP Conf. Proc. 3073, 100007 (2024) https://doi.org/10.1063/5.0193885

Abstract ∨	View article	🗎 PDF

Integration of methanol synthesis and its dehydration using mixed catalysts: Kinetic study from batch process 🛒

Puji Andini; Aisyah Ardy; Melia Laniwati; Jenny Rizkiana; Herri Susanto

AIP Conf. Proc. 3073, 100008 (2024) https://doi.org/10.1063/5.0199197

Abstract ∨	View article	🗎 PDF

CHEMICAL ENGINEERING EDUCATION

Conceptualization and implementation plan of freedom curricula with project-based learning for industrial chemistry major in vocational high school 🛒

Christian Aslan; Ardiyan Harimawan; Dian Shofinita; Vita Wonoputri;
Muhammad Helmi Risansyauqi; Agus Tendi Ahmad Bustomi; Jenny